ELSEVIER

Journal of Alloys and Compounds 446–447 (2007) 733–737

Journal of ALLOYS AND COMPOUNDS

www.elsevier.com/locate/jallcom

Preparation of Ni–Al alloys at reduced temperature for fuel cell applications

Hyung Chul Ham, Anatoly P. Maganyuk, Jonghee Han, Sung Pil Yoon,
Suk Woo Nam*, Tae-Hoon Lim, Seong-Ahn Hong

Fuel Cell Research Center, Korea Institute of Science and Technology, Seoul 136-791, Republic of Korea

Received 31 October 2006; received in revised form 15 February 2007; accepted 15 February 2007

Abstract

Ni–Al alloys have been fabricated from the physical mixture of nickel and aluminum powders at temperatures below the melting point of aluminum using $AlCl_3$ vapor as an activator. Pure Ni_3Al intermetallic compound has been synthesized from the Ni–Al powder mixtures containing 15 wt% aluminum at 600 °C. From the powder mixture containing 5 wt% aluminum, a compound consisting of Ni–Al solid solution and Ni_3Al was produced at 600 °C, but this compound was converted entirely to a Ni–Al solid solution after annealing at 700 °C. The particle size and morphology of the Ni–Al solid solution were not greatly different from original nickel powders. It was observed that oxidation resistance was significantly enhanced by alloying of nickel with aluminum. The Ni–Al alloys synthesized in this study can be used as anode materials for high-temperature fuel cells which need improved resistance toward creep, sintering and redox cycling.

Keywords: Intermetallics; Gas–solid reactions; X-ray diffraction; High temperature alloys; Thermal analysis

1. Introduction

Ni–Al alloys have been mainly applied as anode materials for molten carbonate fuel cells (MCFCs). Alloying of nickel anodes with aluminum provides enhanced creep strength and sintering resistance, resulting in excellent mechanical and chemical stability during the long-term operation of the fuel cell at temperatures around 650 °C [1]. Ni–Al anodes with aluminum contents less than 15 wt% have been extensively studied for MCFCs [2–6]. Since the solubility limit of aluminum in nickel at 650 °C is about 5 wt%, a Ni–Al system containing less aluminum than the limit exists in the equilibrium state as a solid solution, whereas the system with more aluminum becomes a mixture of Ni_3Al intermetallic compound (Ni–13.3 wt% Al) and Ni–5 wt% Al solid solution [4]. Ni–Al alloy was also suggested as an alternative cathode material for MCFC [7,8]. Ni–Al alloys with Al concentrations of 5 at% (2.4 wt% Al) and 15 at% Al (7.5 wt% Al) were investigated to reduce the dissolution rate of the cathode, and thus to improve the lifetime of the MCFC. In catalytic applications, Ni–Al alloys with relatively high aluminum contents are well known as precursors to prepare highly porous Raney-Ni catalysts for various reactions [9–11]. Recently Ni_3Al has been examined as a catalyst to produce hydrogen from methanol for fuel cell applications [12,13].

Preparation of the Ni–Al alloy normally involves melting of nickel and aluminum at high temperature around 1400 °C. Synthesis of Ni–Al alloy without melting of nickel and aluminum is more desirable to reduce the cost of alloy production. Previously, porous Ni–Al anodes have been prepared from mixtures of elemental powders at 1100–1200 °C [2–4], but the temperature is still too high to reduce the cost of alloy preparation significantly. Combustion synthesis or reaction synthesis has also been devised as an economic process to produce of Ni–Al intermetallic materials [14].

The purpose of this study is to investigate the Ni–Al alloy formation below the melting point of aluminum (660 °C). To this end, aluminum chloride ($AlCl_3$) is adopted as an activator for the formation of Ni–Al alloy powders. When mixtures of aluminum and nickel powders are exposed to $AlCl_3$ vapor, aluminum in the mixtures can react with $AlCl_3$ to produce AlCl and $AlCl_2$, which

---

* Corresponding author. Tel.: +82 2 958 5274; fax: +82 2 958 5199.
E-mail address: swn@kist.re.kr (S.W. Nam).

0925-8388/$ – see front matter © 2007 Elsevier B.V. All rights reserved.
doi:10.1016/j.jallcom.2007.02.096

react with nickel to form Ni–Al deposits on the nickel surface. The chemical reaction for formation of Ni–Al alloy powders can be expressed as follows:

$$AlCl_3(g) + Al(s) \rightarrow AlCl(g) + AlCl_2(g) \quad (1)$$

$$AlCl(g) + AlCl_2(g) + Ni(s) \rightarrow Ni\text{–}Al(s) + AlCl_3(g) \quad (2)$$

The process is similar to the conventional pack cementation for diffusion coating of aluminum on high-temperature alloys, where the powder pack consists of aluminum as a deposition source, halide compound as an activator and alumina as an inert filler. Since the formation of aluminide coating depends on the partial pressure of AlCl and $AlCl_2$ as shown in Eq. (2), a temperature much higher than 700 °C is needed in order to provide a high partial pressure of AlCl and $AlCl_2$ from the reaction of aluminum and a halide activator [15–19]. A recent study on pack cementation conditions has shown that the temperature of the aluminde coating can be reduced to 650 °C by directly applying $AlCl_3$ as an activator [20].

In this study, we have prepared Ni–Al alloy powders from a mixture of Ni and Al elemental powders using $AlCl_3$ as an activator. The effect of reaction temperatures on alloy formation has been thoroughly investigated. In addition, oxidation behavior of the Ni–Al alloy powders was examined.

2. Experimental

Configuration of the reaction system to prepare Ni–Al alloy is shown in Fig. 1. Powders of chain-shape nickel (Inco 255) with an average particle size of 6.3 μm and spherical-shape aluminum (Alfa Aesar) with a size of 4.2 μm were mixed and subject to ball milling for 24 h. The aluminum content of 5 or 15 wt% was used in the mixture. The mixed powders were put into an alumina dish and placed in a reactor made of stainless steel. Then the reactor was heated up inside a furnace to a desired reaction temperature under the continuous flow of hydrogen for 5 h. Then hydrogen was switched to a packed bed of $AlCl_3$ (Junsei Chemical) in a quartz tube where $AlCl_3$ vapor was produced by sublimation at constant temperature of 130 °C. To remove water vapor and oxygen in the hydrogen stream, traps were used before hydrogen entering the packed bed of $AlCl_3$. The reactor was maintained at 400, 500 or 600 °C for 6 h while supplying $AlCl_3$ in hydrogen. After the reaction, supply of $AlCl_3$ was stopped and the reactor was slowly cooled down to room temperature.

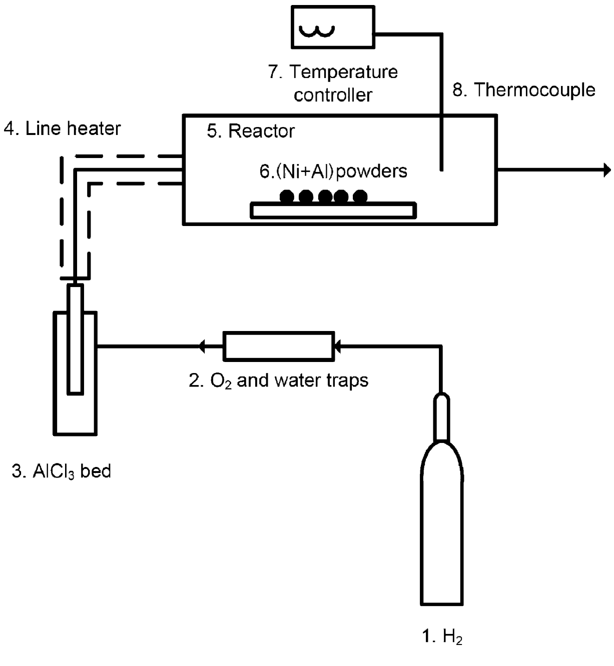

Fig. 1. Configuration of a reaction system for Ni–Al alloy formation.

The phases and morphologies of Ni–Al alloy were characterized by an X-ray powder diffractometer (XRD, Rint/DMAX 2500-Rigaku) and a scanning electron microscope (SEM, HITACHI S-4100). The content of aluminum in the product was measured by an inductively coupled plasma-atomic emission spectrometer (ICP-AES, Leeman Prodigy). The oxidation behaviors of the alloys were examined by a thermogravimetric analyzer (TGA, Ta Instruments) under the flow of air at a ramp rate of 10 °C/min. Particle sizes of the alloy powders were measured with a centrifugal particle size analyzer (Horiba CAPA 300).

3. Results and discussions

3.1. Effect of reaction temperature

Fig. 2 shows evolution of XRD patterns with the increase of reaction temperature for the powder mixture containing 5 wt% aluminum. It can be clearly seen that the reaction to form Ni–Al alloys does not take place at 400 °C since the XRD patterns of the samples from the 400 °C reaction are the same as those of the original sample before the heat treatment. At a reaction temperature of 500 °C, peaks of metallic aluminum decrease and peaks corresponding to Ni_3Al and γ-phase Ni–Al solid solution are detected, indicating that limited reaction takes place. At a reaction temperature of 600 °C, peaks of aluminum are not detected and compounds consisting of Ni_3Al and Ni–Al solid solution are detected. This means that aluminum contained in the original mixture was completely consumed to form Ni–Al alloy powders.

According to the phase diagram of the Ni–Al binary system [14], the solubility of aluminum in nickel depends on temperature. At around 600 °C, the solubility of aluminum is about 4.5 wt%. So the sample containing 5 wt% aluminum becomes two phases comprised of Ni_3Al intermetallic compound and Ni–Al solid solution due to limited solubility of aluminum in nickel. The Vegard law allows an approximate prediction of the

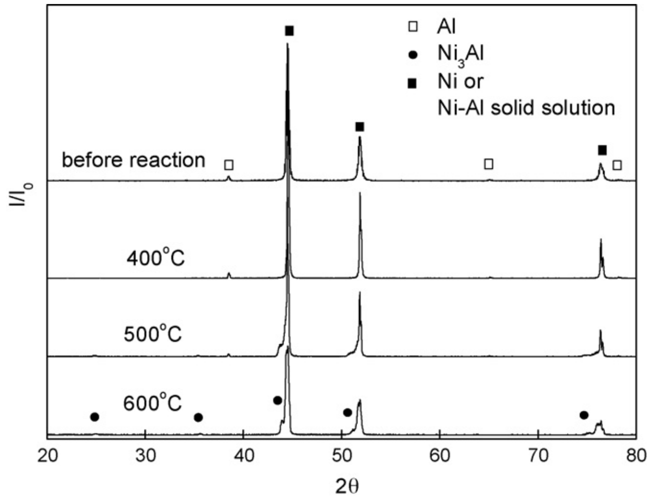

Fig. 2. Evolution of XRD patterns with respect to the reaction temperature for the Ni–Al sample containing 5 wt% aluminum.

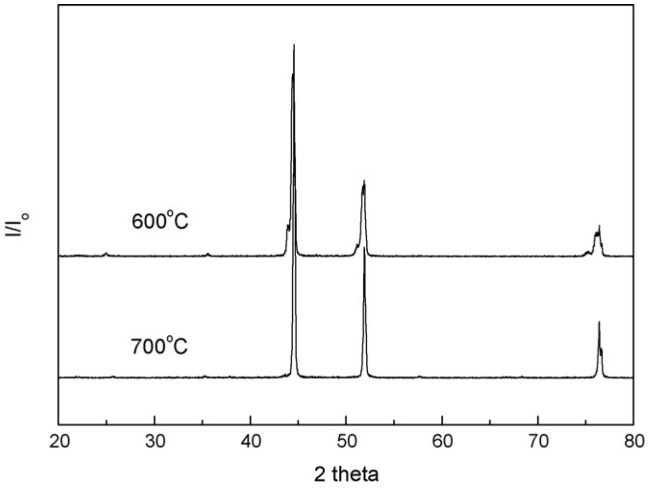

Fig. 3. Effect of annealing on XRD patterns of the Ni–Al sample containing 5 wt% aluminum.

amount of aluminum in Ni–Al solid solution [21]. The amount of aluminum calculated is 2.5 wt% in Ni–Al solid solution, which is lower than the solubility of aluminum in nickel at 600 °C. This may be attributed to the slow cooling process that affects the solubility of aluminum as the temperature decreases from 600 to 25 °C. The sample obtained at a reaction temperature of 600 °C was further heat treated at 700 °C under hydrogen flow without addition of $AlCl_3$ for 6 h. Fig. 3 shows the XRD peaks of the sample before and after the heat treatment at 700 °C, indicating that Ni–5 wt% Al solid solution can be formed by annealing at higher temperature.

Fig. 4 represents the evolution of XRD patterns with the increase of reaction temperature for the powder mixture containing 15 wt% aluminum. The results illustrate that significant reaction forming Ni_3Al intermetallic compound occurs at 500 °C, and a pure cubic phase of Ni_3Al can be synthesized at 600 °C. The lattice parameters for the unit cell of Ni_3Al prepared in this study are in good agreement with the known lattice parameters for Ni_3Al ($a = 3.572$). The content of aluminum in Ni_3Al compound measured by ICP is about 13.5 wt%, which is close to the theoretical value of 13.3 wt%, but is somewhat lower than the content of aluminum used in the original sample (15 wt%). The difference may be due to the some loss of aluminum powders that may adhere to the surface of the ball mill bottle. From the phase diagram of the binary Ni–Al system, it is expected that the mixture of Ni–13.5 wt% Al powders can be transformed to form pure Ni_3Al intermetallic compound powders.

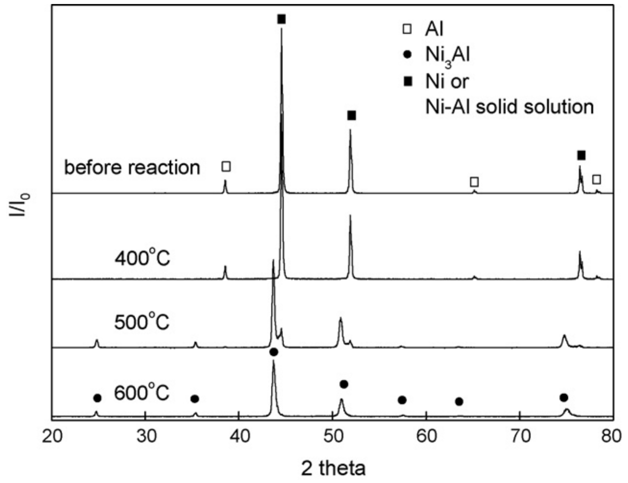

Fig. 4. Evolution of XRD patterns with respect to the reaction temperature for the Ni–Al sample containing 15 wt% aluminum.

Fig. 5 shows SEM images of the original mixture of elemental powders and Ni–Al alloy samples obtained at 600 °C. In Fig. 5(a), the spherical particles with smooth surfaces are aluminum and the others are nickel powders. In Fig. 5(b) and (c),

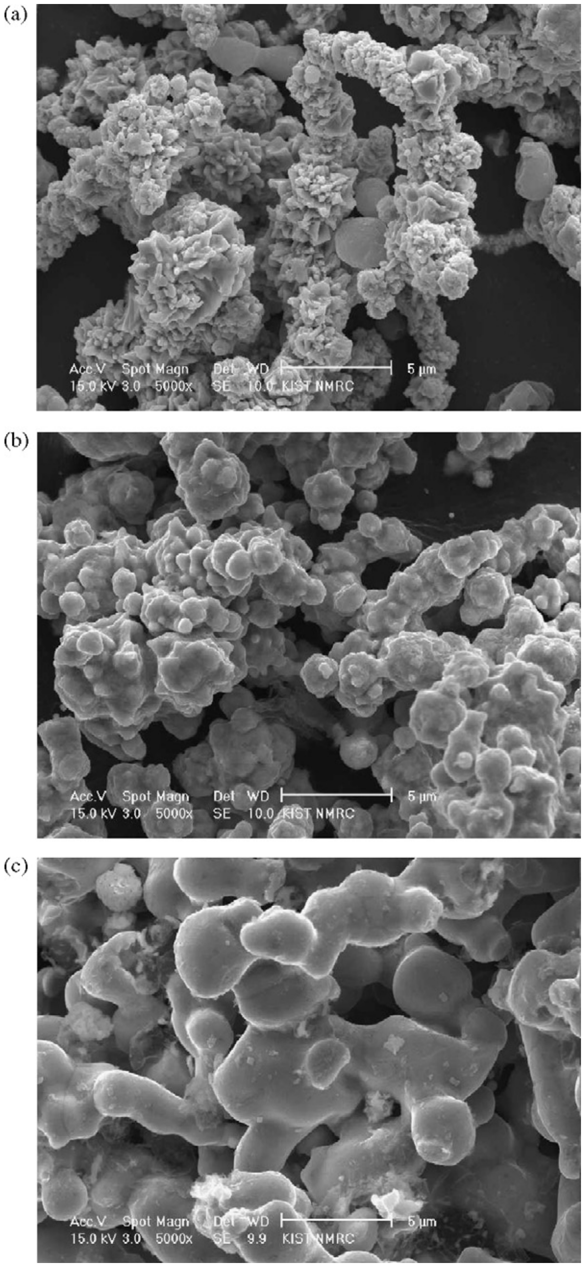

Fig. 5. SEM images of Ni–Al powders: (a) original powder mixture before the reaction; (b) Ni_3Al/Ni–Al solid solution prepared at 600 °C; (c) Ni_3Al intermetallic compound prepared at 600 °C.

Table 1
Average particle size of Ni–Al alloy powders prepared in this study

Samples	Median diameter (μm)
Ni elemental powders (Inco 255)	6.3
Al elemental powders (Alfa Aesar)	4.2
Ni_3Al/Ni–Al solid solution two-phase alloy powders	9.5
Ni_3Al intermetallic compound powders	7.1

aluminum having a smooth surface was not observed, confirming that Al is consumed to form Ni–Al powders. For the sample containing 5 wt% aluminum, Ni–Al powders maintain the original shape of chain-like nickel as shown in Fig. 5(b), whereas, for the sample containing 15 wt% aluminum, the particles look expanded after alloy formation.

Table 1 shows the average particle size of the Ni–Al alloy powders in comparison with the original elemental powders, demonstrating that the size of the produced two-phase alloy powders or Ni_3Al powders is not largely different from original particle size of the nickel.

3.2. Alloy formation process

In this study, $AlCl_3$ vapor was introduced as an activator for the formation of Ni–Al alloy from the mixture of nickel and aluminum powders. The alloy formation consists of a number of transportation and reaction steps involving: (1) diffusion of $AlCl_3$ vapor from the bulk stream to the aluminum surface, (2) reaction of $AlCl_3$ vapor with aluminum to produce active AlCl and $AlCl_2$ vapors, (3) diffusion of AlCl and $AlCl_2$ species to the surface of nickel, (4) reaction of AlCl and $AlCl_2$ with nickel to form Ni–Al compounds, and (5) inward diffusion of aluminum in nickel powder. Further investigation is needed to elucidate the exact mechanism and rate-determining steps in alloy formation. Yet, the results so far indicate that rates of diffusion and reaction in Ni–Al alloy formation are relatively fast compare to those in the conventional pack cementation process in that a reaction temperature of 600 °C is enough to form Ni–Al solid solution and Ni_3Al intermetallic compound. It was observed qualitatively that purity of hydrogen affects the alloying temperature significantly. This result indicates that diffusion of $AlCl_3$ vapor to the aluminum surface and subsequent diffusion of AlCl and $AlCl_2$ from the aluminum surface through Al_2O_3 films formed on the aluminum may be the rate-limiting steps.

3.3. Oxidation resistance of Ni–Al alloy

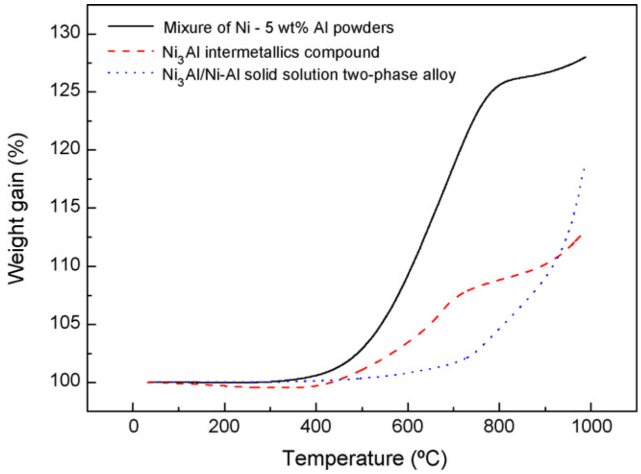

Fig. 6. Oxidation behavior of the Ni–Al compounds obtained at 600 °C in comparison with that of the physical mixture of nickel and aluminum.

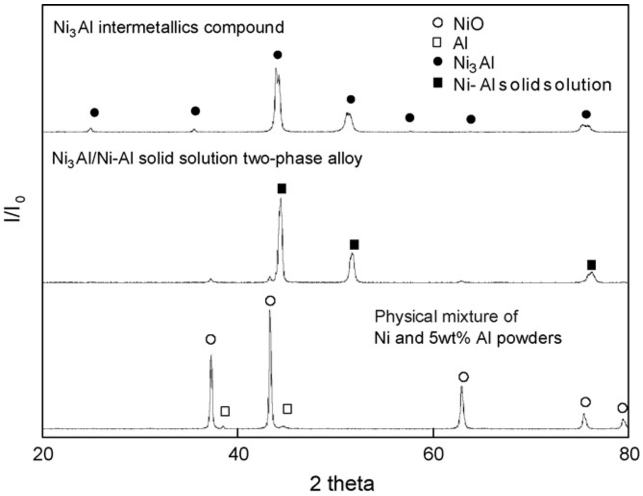

Fig. 7. XRD patterns of the Ni–Al compounds after oxidation in air at 600 °C for 24 h.

Fig. 6 shows the oxidation behaviors of the Ni–Al compounds obtained at 600 °C in comparison with that of the physical mixture of nickel-5 wt% aluminum. The results demonstrates that oxidation resistance of Ni_3Al/Ni–Al solid solution or pure Ni_3Al intermetallic compound is much higher than that of a physical mixture of nickel and aluminum. Fig. 7 shows XRD patterns obtained after oxidation of the samples at 650 °C under air flow for 24 h. Ni_3Al intermetallic compound was not affected by oxidation treatment, whereas a small amount of NiO appeared in Ni_3Al/Ni–Al solid solution, indicating that oxidation occurred on the surface of the solid solution, although the rate was low. Compared with the physical mixture of nickel and aluminum, however, Ni–Al alloy shows much higher oxidation resistance. In the real operation of high-temperature fuel cells, reduction and reoxidation of Ni-based anodes might occur due to a lack of fuel gas, sealant damage or system shutdown [22–24]. Ni–Al alloy with improved redox resistance may be applied as an alternative to current Ni-based anodes to enhance the lifetime of the fuel cells.

4. Conclusions

Pure Ni_3Al intermetallic compound as well as two-phase alloy powders of Ni_3Al and Ni–Al solid solution have been prepared from the physical mixture of nickel and aluminum powders at a reduced temperature of 600 °C. $AlCl_3$ vapor used as an activator was effective in reducing the temperature of alloy formation. Particle size and morphology of the Ni–Al solid solution were close to those of nickel powders. Alloying of nickel with aluminum greatly improves the oxidation resistance. The Ni–Al alloy synthesized in this study can be used as anode materials for high-temperature fuel cells which need improved resistance toward creep, sintering and redox cycling.

Acknowledgements

This work was financially supported by Korea Institute of Science and Technology and Ministry of Commerce, Industry and Energy in Korea.

References

[1] M. Farooque, H.C. Maru, J. Power Sources 160 (2006) 827–834.
[2] G. Kim, Y. Moon, D. Lee, J. Power Sources 104 (2002) 181–189.
[3] D. Kim, I. Lee, H. Lim, D. Lee, J. Power Sources 109 (2002) 347–355.
[4] D. Lee, I. Lee, S. Chang, Electrochim. Acta 50 (2004) 755–759.
[5] Y.-S. Kim, H.-S. Chun, J. Power Sources 84 (1999) 80–86.
[6] J.-H. Wee, D.-J. Song, C.-S. Jun, T.-H. Lim, S.-A. Hong, H.-C. Lim, K.-Y. Lee, J. Alloys Compd. 390 (2005) 155–160.
[7] M. Mohamedi, Y. Hisamitsu, K. Kihara, T. Kudo, T. Itoh, I. Uchida, J. Alloys Compd. 315 (2001) 224–233.
[8] T. Kudo, Y. Hisamitsu, K. Kihara, M. Mohamedi, I. Uchida, J. Appl. Electrochem. 32 (2002) 179–184.
[9] S. Tanaka, N. Hirose, T. Tanaki, Y.H. Ogata, J. Electrochem. Soc. 147 (2000) 2242–2245.
[10] B. Liu, M. Qiao, J.-F. Deng, K. Fan, X. Zhang, B. Zong, J. Catal. 204 (2001) 512–515.
[11] H. Hu, F. Xie, Y. Pei, M. Qiao, S. Yan, H. He, K. Fan, H. Li, B. Zong, X. Zhang, J. Catal. 237 (2006) 143–151.
[12] Y. Xu, S. Kameoka, K. Kishida, M. Demura, A. Tsai, T. Hirano, Intermetallics 13 (2005) 151–155.
[13] D.H. Chun, Y. Xu, M. Demura, K. Kishida, D.M. Wee, T. Hirano, J. Catal. 243 (2006) 99–107.
[14] K. Morsi, Mater. Sci. Eng. A 299 (2001) 1–15.
[15] H.J. Lin, W.P. Sun, M.H. Hon, Thin Solid Films 156 (1988) 259–264.
[16] N. Voudouris, Ch. Christoglou, G.N. Angelopoulos, Surf. Coat. Technol. 141 (2001) 275–282.
[17] Z.D. Xiang, J.S. Burnell-Gray, P.K. Datta, J. Mater. Sci. 36 (2001) 5673–5682.
[18] C. Houngninou, S. Chevalier, J.P. Larpin, Appl. Surf. Sci. 236 (2004) 256–269.
[19] J.T. John, R.S. Srinivasa, P.K. De, Thin Solid Films 466 (2004) 339–346.
[20] Z.D. Xiang, P.K. Datta, Acta Mater. 54 (2006) 4453–4463.
[21] B.D. Cullity, Elements of X-ray Diffraction, 3rd ed., Prentice Hall, 2001, p. 339.
[22] D. Waldbillig, A. Wood, D.G. Ivey, J. Power Sources 145 (2005) 206–215.
[23] J. Malzbender, E. Wessel, R.W. Steinbrech, Solid State Ionics 176 (2005) 2201–2203.
[24] Y. Zhang, B. Liu, B. Tu, Y. Dong, M. Cheng, Solid State Ionics 176 (2005) 2193–2199.